INFECTION AND IMMUNITY, Aug. 1995, p. 3143–3150
0019-9567/95/$04.00+0

Vol. 63, No. 8

Quantitative Comparison of Clumping Factor- and Coagulase-Mediated *Staphylococcus aureus* Adhesion to Surface-Bound Fibrinogen under Flow

RICHARD B. DICKINSON,[1]* JENNIFER A. NAGEL,[2] DAMIEN McDEVITT,[3] TIMOTHY J. FOSTER,[3] RICHARD A. PROCTOR,[4] AND STUART L. COOPER[2]

Department of Chemical Engineering, University of Florida, Gainesville, Florida[1]; Department of Chemical Engineering, University of Delaware, Newark, Delaware[2]; Department of Microbiology, Moyne Institute, Trinity College, Ireland[3]; and Departments of Medicine and of Medical Microbiology and Immunology, University of Wisconsin Medical School, Madison, Wisconsin[4]

Received 7 November 1994/Returned for modification 24 February 1995/Accepted 9 May 1995

The contributions of clumping factor and coagulase in mediating *Staphylococcus aureus* adhesion to surface-adsorbed fibrinogen have been quantified by using a new methodology and analysis. The attachment or detachment kinetics of bacteria were directly observed in a radial flow chamber with a well-defined laminar flow field and a spatially varying shear rate and were quantified by recursively scanning the chamber surface and counting cells via automated video microscopy and image analysis with a motorized stage and focus control. Intrinsic rate constants for attachment or detachment were estimated as functions of shear rate for the wild-type Newman strain of *S. aureus* and for mutants lacking clumping factor, coagulase, or both proteins on surfaces coated with plasma, fibrinogen, or albumin. Clumping factor, but not coagulase, increased the probability of attachment and decreased the probability of detachment of *S. aureus* on plasma-coated surfaces; however, both clumping factor and, to a lesser extent, coagulase increased the probability of attachment on the purified-fibrinogen-coated surface. All mutants were resistant to detachment on the purified-fibrinogen-coated surface, suggesting the possibility of an additional adhesion mechanism which was independent of coagulase or clumping factor and effective only for fully attached cells. Together, these results suggest that the presence of clumping factor plays the primary role in enhancing adhesion to surfaces with adsorbed fibrinogen, not only by enhancing the probability of cell attachment but also by increasing the strength of the resulting adhesion.

Infection of implanted or intravascular devices is a frequently occurring and potential life-threatening complication. Bacterial adhesion to biomaterial surfaces is believed to be an essential step in the pathogenesis of these infections (8, 12, 17, 18, 40); however, the molecular and physical interactions that govern bacterial adhesion to biomaterials have not been studied in detail. Both specific (i.e., receptor-ligand) and nonspecific (i.e., colloidal-type) interactions may play a role in the ability of the cell to attach to (or resist detachment from) the biomaterial surface (8, 40).

Within the intravascular space, adhesion of bacteria occurs under flow conditions; therefore, the fluid shear rate on the biomaterial surface likely plays a role in attachment and detachment of bacteria, in addition to the role played by cell-material interactions. Physiological shear rates can range between 40 and 2,000 s^{-1} for stable laminar flow in vessels, with much higher shear rates possible in turbulent flow or at vessel entrances and bifurcations (16). Stable adhesion requires both attachment and resistance to detachment under these shear conditions; therefore, the sensitivity of cell attachment and detachment to the shear rate is also an important factor in determining the likelihood of cell adhesion, colonization, and embolism.

Staphylococcus aureus is a pathogen that is frequently involved in device-centered infections and that has been shown to bind specifically to a variety of plasma proteins (21, 22, 28, 32), including fibrinogen (2, 6, 21, 22, 25, 29, 32) and fibronectin (22, 24, 34, 39). Fibrinogen is a major blood protein responsible for the clumping of plasma in the presence of *S. aureus* (19, 20). Two cell surface-associated proteins on *S. aureus* have been implicated in binding to fibrinogen: clumping factor (CF) (5, 9, 14, 26, 37, 38) and coagulase (Coag) (2, 13, 27). However, whether cell surface-associated Coag influences cell adhesion to solid-phase fibrinogen is an open question. Recent genetic analyses of Coag-negative and CF-negative mutants of *S. aureus* have demonstrated that CF and Coag are distinct molecules (27) and that CF is the primary molecule involved in clumping with fibrinogen in solution and in adhesion on surface-bound fibrinogen (26). Nevertheless, the attachment of a CF-negative (Coag-positive) mutant on surface-bound fibrinogen increased in a dose-dependent manner, but to a lesser extent than that of the CF-positive wild type (26). These studies have helped elucidate the molecular mediators of *S. aureus* adhesion on fibrinogen, but several questions remain. Do CF and/or Coag increase the likelihood of cell attachment or the resistance to detachment, or both, under defined flow conditions? What are the relative contributions of these molecules in increasing cell attachment or resistance to detachment in comparison with each other and with other factors? How do CF- and Coag-mediated attachment, or resistance to detachment, depend on shear stress? Do cell attachment and detachment behaviors on purified-fibrinogen-coated surfaces correlate with those on plasma-coated surfaces?

Previous studies of staphylococcal adhesion to biomaterials have been limited because shear force either was not present or was ill-defined. A few studies have examined adhesion un-

* Corresponding author. Mailing address: Department of Chemical Engineering, University of Florida, P.O. Box 116005, 227 CHE Bldg., Gainesville, FL 32611. Phone: (904) 392-0898. Fax: (904) 392-9513. Electronic mail address: dickinso@che.ufl.edu.

der well-defined flow conditions, but only end point data were available, providing only a single snapshot of a dynamic process and thus limiting the validity and strength of the conclusions reached.

This study addresses the above-mentioned questions by using a novel methodology and analysis to quantitatively characterize bacterial attachment and detachment kinetics on surfaces as functions of fluid shear stress (11). Attachment and detachment kinetics were directly observed on the collector surface of a radial flow chamber (RFC), which was exposed to a radially varying shear stress. The cell density on the surface was measured as a function of time and radial position by recursively scanning and counting attached cells in multiple fields via automated video microscopy and image analysis with a motorized stage and focus control. Solutions of mathematical models for attachment and detachment kinetics were fitted to the experimental data for the cell density to estimate intrinsic rate constants for attachment or detachment. These rate constants have direct physical interpretations and are intrinsic in that they depend only on the local fluid dynamics and local interactions between the cell and the surface and not on assay-specific global parameters such as experiment duration, assay dimensions, cell concentration, etc. The analysis further yielded estimates of intrinsic parameters that reflect the sensitivities of the attachment and detachment probabilities to the shear rate and reflect the heterogeneity in adhesion strength (i.e., resistance to detachment under flow) among the attached cell population.

This methodology and analysis was applied to quantify the attachment and detachment behavior of the Newman strain of *S. aureus* and mutants lacking CF, Coag, or both proteins on surfaces coated with fibrinogen, albumin, or plasma. The results show that only CF enhanced the probability of attachment and decreased the adhesion strength of *S. aureus* on plasma-coated surfaces. However, on the purified-fibrinogen-coated surfaces, CF and, to a lesser extent, Coag both enhanced the probability of attachment. Furthermore, all mutants were highly resistant to detachment on fibrinogen-coated surfaces, suggesting the possibility of an adhesion mechanism that was independent of Coag and CF and effective only for fully attached cells. In general, bacteria that were most resistant to detachment also showed the least sensitivity to shear rate for both the attachment and detachment processes and showed greater heterogeneity among the attached cell population with respect to adhesion strength. These quantitative results suggest that it is primarily specific binding of CF to fibrinogen that enhances the affinity of cells for the surface, by both increasing attachment and decreasing detachment on surfaces with adsorbed fibrinogen.

MATERIALS AND METHODS

Buffered medium. The fluid medium used in all flow experiments was Dulbecco's phosphate-buffered saline (Gibco BRL, Gaithersburg, Md.), supplemented with 0.1 mg of $MgCl_2$ per ml and 0.1 mg of $CaCl_2$ per ml, at pH 7.35. (Hereafter, this solution will be referred to as buffer.) The buffer was filtered and degassed before use.

Bacterial strains and growth media. The wild-type *S. aureus* Newman strain and mutants of it were used. The Coag-negative mutant DU5855 was obtained by site-directed deletion of all but about 50 bp of the *coa* gene, which was marked with the tetracycline resistance determinant (Δ*coa*::Tc^r) (27). The CF-negative mutant DU5852 was obtained by transposon (Tn*917*) insertion into the fibrinogen receptor gene (*clfA*::Tn*917*) (26). The mutant deficient in both CF and Coag, DU5858, was obtained by phage 85 transduction of the Δ*coa*::Tc^r mutation into DU5852. Working cultures were maintained on Mueller-Hinton agar plates. Before use, bacteria were grown overnight in tryptic soy broth, washed twice in buffer, lightly sonicated to separate any clumped cells, and then resuspended in buffer at a concentration of 5×10^7 cells per ml for attachment experiments or 2×10^8 cells per ml for detachment experiments. Cell densities remained below 1% surface coverage in all experiments, which, as indicated by the data (see Fig. 2), was sufficiently low so as to not significantly influence the further attachment of cells. Very few cell aggregates were observed in the experiments.

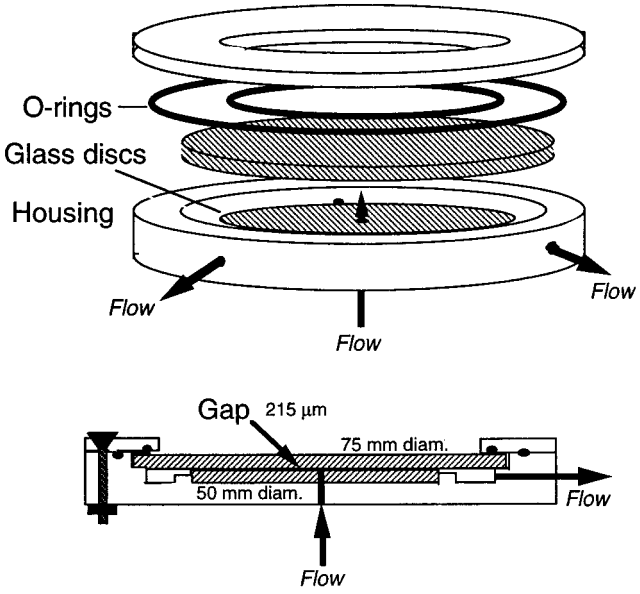

FIG. 1. Schematic diagram of the RFC. A Plexiglas chamber housed two optically flat glass discs separated by a thin gap. One disc was fixed to the chamber with the inlet port bored in its center, and the other disc could be removed and treated. The fluid flowed in through the center of the fixed disc, flowed out radially between the two discs, collected in a surrounding trough, and then flowed out through three equally spaced exit ports. The fluid dynamics between the discs were well defined, such that the shear stress on the surface was inversely proportional to the radial position.

Proteins. Whole fresh human platelet-poor plasma was prepared from blood samples from healthy volunteers by centrifuging blood anticoagulated with ACD (citric acid, 5 mM [final concentration]; sodium citrate, 10 mM; and glucose, 15 mM) for 15 min at $1,500 \times g$; the plasma was pooled, aliquoted, and stored at −70°C. Human albumin (fraction V, 96 to 99% pure) was purchased from Sigma Chemical Co. (St. Louis, Mo.). Human fibrinogen was purchased from Sigma Pharmaceuticals (St. Louis, Mo.) and further purified with a gelatin–Sepharose 4B (Pharmacia, Piscataway, N.J.) column to remove residual fibronectin. Purity was confirmed by sodium dodecyl sulfate-polyacrylamide gel electrophoresis.

RFC. A schematic diagram of the RFC is shown in Fig. 1. The operation of the RFC and a description of the associated apparatus are detailed elsewhere (11) and are summarized here. The RFC consisted of two optically flat glass discs (Melles Griot, Irving, Calif.) separated by a thin gap (215 ± 5 μm) and housed in a Plexiglas chamber. One disc (50-mm diameter, 3-mm thickness) was permanently cemented to the chamber and was bored with a 0.080-in. (ca. 2.03-mm)-diameter inlet port through its center. The second disc (75-mm diameter, 3-mm thickness) was removable and could be pretreated to give conditions of interest. The surface of this disc was the collector surface (i.e., where attachment or detachment was observed).

The fluid dynamics in the RFC have been well characterized elsewhere (15, 30). For a given volumetric flow rate, the shear rate on the collector surface (S) was inversely proportional to the radial position from the inlet port (r) and was calculated from the gap width (h) and the volumetric flow rate (Q) by the relation

$$S = \frac{3Q}{\pi r h^2} \quad (1)$$

S and r are used interchangeably hereafter, given equation 1 and that h and Q are known.

In attachment experiments, cells in suspension (5×10^7 cells per ml) flowed through the RFC at a flow rate of 2 ml/min, corresponding to shear rates ranging between approximately 35 and 200 s^{-1} in the observed microscope fields. Cell detachment experiments were conducted by first injecting the cell suspension (2×10^8 cells per ml) into the RFC and allowing the bacteria to settle for 10 min before initiating flow. To induce a measurable rate of detachment for all conditions, a significantly higher flow rate of 75 ml/min was used, which corresponded to a shear rates ranging from approximately 1,500 to 7,000 s^{-1}.

Disc preparation. Before being used in adhesion experiments, discs were incubated overnight in buffer and then pretreated in one of three ways: (i) 1 h in 0.02 mg of fibrinogen per ml in buffer and then 1 h in 0.5% human albumin in

TABLE 1. Parameters and variables

Parameter or variable	Symbol	Unit
Experimental variables		
Cell surface density	c_s	Cells/cm^2
Shear rate	S	s^{-1}
Time	t	min
Radial position	r	cm
Rate of attachment	R	Cells/cm^2/min
Attachment parameters		
Effective attachment rate constant	k_{eff}	cm/min
True attachment rate constant	k_+	cm/min
Base attachment rate constant	k_{+0}	cm/min
Shear sensitivity coefficient	δ	s
Detachment parameters		
Detachment rate constant	k_-	min^{-1}
Free energy of adhesion	E	ergs
Mean free energy of adhesion	$\bar{E}$	ergs
Mean-energy detachment rate constant	$\bar{k}_-$	min^{-1}
Adhesion energy heterogeneity parameter	σ	None
Shear sensitivity coefficient of detachment	δ_d	s

buffer (to block any exposed glass not adsorbed with fibrinogen with nonadhesive protein), (ii) 1 h in buffer and then 1 h in 0.5% human albumin in buffer, or (iii) 2 h in 1% platelet-poor plasma. (Hereafter, surfaces with these treatments are referred to as FG, HSA, and PPP, respectively.) During treatment, the discs were swirled in the protein solutions on a rotating platform. After treatment, the protein solution was replaced with buffer.

Automated video microscopy. An automated video microscopy and image analysis system was used to rapidly and recursively count attached bacteria in multiple fields over the collector surface. This system consisted of a Nikon Diaphot inverted microscope with a motorized stage (0.1-μm spatial resolution) and focus control (LUDL Electronics Products Ltd., Hawthorne, N.Y.), a Dage NC-65 Newvicon video camera (Dage MTI, Inc., Michigan City, Ind.), a Sony SVO-9500MD videocassette recorder with a Trinitron color monitor (Sony Medical Systems, Montvale, N.J.), and a Gateway2000 4DX2-66E minicomputer (Gateway2000, North Sioux City, S. Dak.) with an OFG frame-grabbing board (640 × 480 pixels) (Imaging Technologies, Bedford, Mass.) and Optimas image analysis software (Bioscan, Inc., Edmonds, Wash.). The videocassette recorder and the motorized stage/focus controller were connected on-line to the minicomputer via RS232C serial connections, and analog video input from the video camera or videocassette recorder was digitized by the frame-grabbing board and processed by Optimas software functions. This system allowed rapid automated microscope field selection, image archiving, and image processing.

One Optimas program recursively scanned 32 fields (four fields azimuthally by eight fields radially) of a wedge-shaped area of the collector surface (approximately 1.5 min per scan) and stored the images on video tape in an automated fashion. A second program then replayed and processed the images to obtain cell counts for each field. The attached-cell density, $c_s(r,t)$, at each radial position r and time t was calculated from the average of cell counts from the four fields at each time increment.

Data analysis. A number of quantitative parameters were estimated from the resultant data for $c_s(r,t)$. These parameters characterize the attachment and detachment kinetics as well as the dependence of these kinetics on shear stress. They are defined so as to be dependent only on local interactions between the cells and the surface and to be independent of global experimental parameters, such as the assay dimensions or experiment duration. Parameter estimation required formulation of mathematical models of attachment, detachment, and convective-diffusive transport of cells in the RFC and subsequent least-squares regression fit of the model solutions to the data for $c_s(r,t)$. The full analysis is detailed elsewhere (11) and summarized here. The symbolic nomenclature used here for parameters and variables is presented in Table 1.

During the attachment experiments, c_s increased linearly with t during attachment for all samples and shear rates measured, implying that the attachment rate (R) at any radial position (r) was constant with time and suggesting that the detachment rate was negligible relative to the attachment rate. $R(r)$ was determined from the slope of $c_s(r,t)$ versus time (t) as estimated by linear least-squares regression (see Fig. 2) and was assumed to be proportional to the cell concentration in suspension near the surface at r (i.e., to the number of cells available for attachment). An effective attachment rate constant (k_{eff}) was obtained at each r by dividing $R(r)$ by the (known) initial cell concentration in suspension. Because fast attachment could lead to a downstream depletion of cells near the collector surface and slow attachment with sedimentation could lead to a downstream accumulation of cells near the collector surface, k_{eff} depended on the global transport and attachment of cells in the chamber. An intrinsic attachment rate constant (k_+) was estimated by dividing $R(r)$ by the actual concentration of cells near the collector surface at r as predicted by the mathematical model. k_+ physically reflects the ability of a cell near the surface to overcome any separating energy barrier and attach to the surface. The model is based on the assumption that k_+ depends exponentially on S; i.e.,

$$k_+ = k_{+0}e^{-\delta S} \tag{2}$$

where k_{+0} and δ are fitted parameters. k_{+0} is the base attachment rate constant, the hypothetical value of k_+ in the absence of shear (i.e., the hypothetical limit of $S \to 0$), and δ is a parameter that reflects the sensitivity of k_+ to shear (hereafter referred to as the attachment shear sensitivity coefficient). Equation 2 is based on the physical assumption that the free energy barrier between attached and unattached states is linearly related to the fluid force on the cell to a first-order approximation (11).

The detachment model assumes that each cell has a probability per unit time of detaching (k_-). On the basis of physical arguments presented elsewhere (11), k_- was assumed to be exponentially related to the energy barrier (E) that the cell must cross to detach (hereafter termed the adhesion energy). To account for apparent statistical variation in E among the attached cell population, E was assumed to have a normal probability distribution with mean $\bar{E}$ and standard deviation σ (scaled to the thermal energy, κT, where κ is Boltzmann's constant and T is the absolute temperature). The intrinsic detachment rate constant was then defined as the value of k_- at the mean adhesion energy, $\bar{E}$, and was termed the mean-energy detachment rate constant, $\bar{k}_- = k_-(\bar{E})$. Because $\ln(\bar{k}_-)$ is proportional to $\bar{E}$, it is a good measure of the cell-surface interaction energy of the attached cell population. σ is measure of the heterogeneity in E among the attached cells, and is hereafter termed the adhesion energy heterogeneity parameter. At any S, the detachment model predicts $c_s(t)$ versus t for given values of $\bar{k}_-$ and σ on the basis of the derived formula

$$c_s(t) = c_{s0}\int_0^\infty e^{-xt}\frac{1}{x\sigma\sqrt{2\pi}}exp\left[\frac{-ln(x/\bar{k}_-)}{2\sigma^2}\right]dx \tag{3}$$

In the limit of no heterogeneity in E (i.e., $\sigma \to 0$), this equation becomes equivalent to the simple exponential decay model; i.e., $c_s = c_{s0}e^{-\bar{k}_- t}$.

Both the attachment and the detachment models have been shown to fit the data well for *S. aureus* attachment and detachment on various surfaces over the range of shear rates considered here (11). The relevant intrinsic parameters (k_{+0} and δ for attachment; $\bar{k}_-$ and σ for detachment) were obtained in each case by fitting the model solutions to the data (i.e., k_{eff} versus S for attachment and c_s versus t for detachment) with nonlinear least-squares regression analyses (36). The reported uncertainties in the parameters are the standard errors in the regression estimates. Significant differences are statistically inferred from a P value of less than 0.05 on the basis of a one-sided Student t test comparison of the parameter estimates (23).

RESULTS

Attachment and detachment kinetics were quantified for the various strains on surfaces coated with albumin, plasma, and purified fibrinogen. Albumin is well known as a nonadhesive protein and was used as a negative control, i.e., the minimally adhesive protein-coated surface. The other two treatments compared adhesion to adsorbed fibrinogen in its purified form and its native plasma form. By quantifying the adhesion of mutants deficient in fibrinogen-binding proteins to plasma-coated surfaces, we also compared the relative role of fibrinogen with that of other plasma proteins in mediating *S. aureus* adhesion.

Below we present data for five measured parameters: attachment and detachment rate constants (k_+ and $\bar{k}_-$, respectively), shear sensitivity parameters for attachment and detachment (δ and δ_d, respectively), and σ, which characterizes the heterogeneity in adhesion energy. Together, these intrinsic parameters quantitatively characterize the shear-dependent attachment and detachment kinetics of the different mutants on the different protein-coated surfaces.

Attachment kinetics. Figure 2 shows examples of attachment kinetic data at an intermediate shear rate of approximately 100 s^{-1}. The attached-cell density, c_s, is plotted versus time for the

wild type (CF^+ $Coag^+$) and the double mutant DU5858 (CF^- $Coag^-$) on the fibrinogen-coated surface (FG) (see Materials and Methods). In each case, c_s increased linearly with time, implying that the attachment rate, R (the slope of c_s versus t), at any radial position was constant with time. This observation was consistent for all measured fields, suggesting that (i) the presence of cells on the surface was sufficiently below saturation so as to not influence the attachment of more cells and (ii) the concentration of suspended cells near the surface at any point was constant with time. In this example, the rate of attachment on FG was much greater for the wild type (CF^+ $Coag^+$) than for DU5858 (CF^- $Coag^-$).

Figure 3 shows examples of data for extrinsic and intrinsic attachment rate constants as functions of the shear rate, S. In this example, the rate constants for DU5855 (CF^+ $Coag^-$) on adsorbed human plasma (PPP) are compared with those for DU5855 on adsorbed human albumin (HSA). The datum points are values of the effective attachment rate constant, k_{eff}, which were calculated from the slopes of c_s versus t at the radial positions corresponding to each S. The solid lines are the mathematical model solutions of k_{eff}, which were fitted to the data to estimate the base attachment rate constant, k_{+0}, and the attachment shear sensitivity coefficient, δ. Together, these parameters define k_+ as a function of S (see equation 1), which is shown by the dashed lines in Fig. 3. δ is the slope of the dashed line on this log-linear plot, and k_{+0} is its intercept at $S = 0$. In the example in Fig. 3, k_+ depended more strongly on S for the slowly attaching HSA surface than for the more rapidly attaching PPP surface, as shown by the larger slope of k_+ and thus the larger value of δ on the HSA surface.

The attachments of the different mutants over the range of shear rates are compared by averaging k_+ over the range of shear rates measured between 35 and 200 s^{-1}. The average value, termed the shear-averaged attachment rate constant, $<k_+>$, is plotted in Fig. 4 for the various mutants and surface conditions (the angle brackets hereafter indicate shear-averaged values). $<k_+>$ was smallest and approximately the same for all mutants, indicating that the HSA surface appropriately serves as a minimally adhesive control surface. $<k_+>$ for the wild type (CF^+ $Coag^+$) was larger on both PPP and FG than on HSA, but $<k_+>$ for DU5858 (CF^- $Coag^-$) was as small on FG as on HSA, suggesting that the probability of cell attachment on FG was enhanced by either CF, Coag, or both. On FG, $<k_+>$ was larger for DU5852 (CF^- $Coag^+$) than for DU5858 (CF^- $Coag^-$), suggesting that the probability of attachment was partially increased by the presence of Coag alone on purified fibrinogen. However, $<k_+>$ on FG was much larger for DU5855 (CF^+ $Coag^-$) than for DU5852 (CF^- $Coag^+$), suggesting that the increase in attachment probability provided by Coag alone was much less than that provided by CF alone. Furthermore, $<k_+>$ on FG was slightly lower for the wild type (CF^+ $Coag^+$) than for DU5855 (CF^+ $Coag^-$), suggesting that Coag in combination with CF did not further increase the probability of attachment beyond that with CF alone and may have, in fact, inhibited attachment.

In contrast to the results for attachment on FG, Coag alone did not appear to increase the attachment probability on PPP, as seen by comparing $<k_+>$ on FG for DU5852 (CF^- $Coag^+$) and DU5858 (CF^- $Coag^-$), or in the presence of CF, as seen by comparing $<k_+>$ on PPP for the wild type (CF^+ $Coag^+$) and DU5855 (CF^+ $Coag^-$). However, CF greatly increased the probability of attachment to PPP, as seen by comparing $<k_+>$ on PPP for DU5855 (CF^+ $Coag^-$) and for DU5858 (CF^- $Coag^-$).

The relationship between k_+ and the shear rate is reflected by the parameters k_{+0} and δ (see equation 2). k_{+0} is the zero-shear baseline value of k_+, and δ measures the sensitivity of k_+ to shear. k_{+0} and δ are plotted for the various conditions in Fig. 5 and 6, respectively. Although the values of $<k_+>$ for both the wild type (CF^+ $Coag^+$) and DU5855 (CF^+ $Coag^-$) were similar on PPP and on FG, the corresponding values for k_{+0} were significantly higher on PPP than on FG. Also, k_{+0} for DU5852 (CF^- $Coag^+$) was not much larger on FG than on HSA, in contrast to the results for $<k_+>$. As shown in Fig. 6, these difference are explained by the markedly lower shear sensitivity of all mutants and the wild type on FG than on PPP and HSA, showing small or even negative values of δ on FG for each cell type. The observation of this effect for the double mutant DU5858 (CF^- $Coag^-$) is inexplicable in terms of Coag and CF alone. Related observations were made with the detachment results, as discussed below. Also apparent in Fig. 6 is the greater shear sensitivity of attachment on HSA than on the other surfaces for all cell types, with the exception of the two CF-negative mutants having similar values of δ on both PPP and HSA. This observation further suggests that the presence of Coag did not modify the attachment behavior of *S. aureus* on PPP.

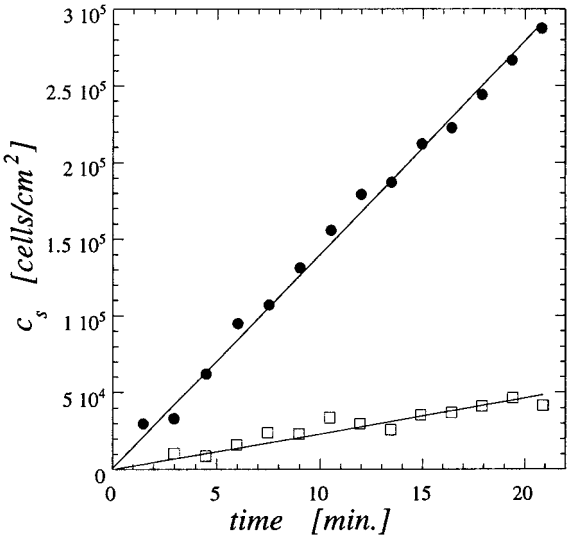

FIG. 2. Attachment kinetics. The surface density of *S. aureus*, c_s, is plotted versus time for the wild-type strain Newman (circles) and the CF-negative, Coag-negative mutant DU5858 (squares) on FG. c_s was calculated from the average number of cells from four microscope fields at a radial position of the flow chamber, corresponding here to a shear rate of approximately 100 s^{-1}. The solid line is a linear least-squares regression fit, the slope of which is the attachment rate, R.

Detachment kinetics. Examples of detachment kinetics are shown in Fig. 7, in which the cell density c_s, is plotted versus time. In this example, c_s(t) is plotted for the wild type (CF^+ $Coag^+$) on FG and on HSA at an intermediate shear rate of approximately 4,000 s^{-1} in each case. As shown here, detachment of the wild type was more rapid on HSA than on FG, indicating that cells were on average more weakly attached to the HSA surface. The solid lines represent the detachment model solution (equation 3) fitted to the experimental data, and the dashed lines represent a simple exponential decay model fitted to the same data. As is apparent in Fig. 7 and demonstrated statistically elsewhere (11), the detachment model that accounts for a possible heterogeneous distribution in adhesion strength among the attached cell population shows a superior fit to the data than the simple exponential decay model, which assumes a homogenous attached cell population.

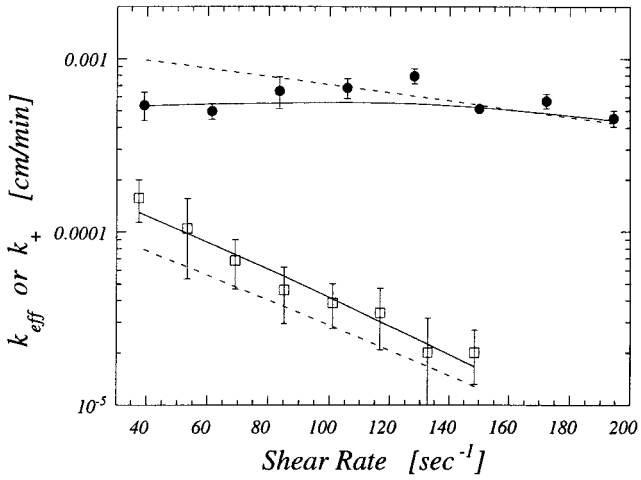

FIG. 3. Dependence of attachment rate constants on shear rate. The effective attachment rate constant, k_{eff}, is defined as the attachment rate, R, divided by the initial concentration of cells in suspension in the radial flow chamber. Here, k_{eff} is plotted for the Coag-negative mutant DU5855 on HSA (squares) or on PPP (circles). The solid lines represent the solutions of the mathematical model for $k_{eff}(S)$, fitted to the data by nonlinear least-squares regression. The regression analysis yields $k_+(S)$, which is shown by the dashed line for each condition.

Heterogeneity is expected when adhesion is governed by a discrete number of molecular interactions because of statistical variation among the cells in the number of bonds in the cell-surface interface (7).

Fitting of the detachment model to experimental data for c_s versus t yielded estimates for the mean-energy detachment rate constant, $\bar{k}_-$, and the adhesion energy heterogeneity parameter, σ. Examples of data for $\bar{k}_-$ versus S are shown Fig. 8, in which values for the wild type (CF^+ $Coag^+$) are plotted for the three different protein coatings. As shown with these data, $\bar{k}_-$ generally increased roughly exponentially with S. Because $\ln(\bar{k}_-)$ was proportional to the mean adhesion energy, $\bar{E}$, this observation suggests that $\bar{E}$ generally decreased linearly with S. In other words, the energy that the cell must overcome to detach was smaller for a larger fluid force on the cell, presumably because of added stress on the molecular bonds between the cell and the surface.

A quantitative comparison of the abilities of the mutants to resist detachment on the different surfaces is shown in Fig. 9.

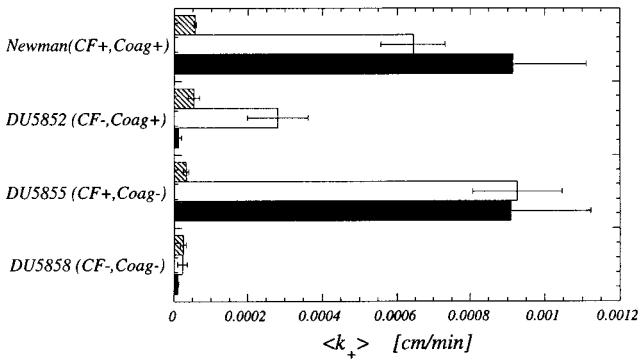

FIG. 4. Shear-averaged attachment rate constants. The intrinsic attachment rate constant, k_+, was averaged over the range of shear rates between 35 and 200 s^{-1} to obtain the shear-averaged attachment rate constant, $<k_+>$, which is plotted here for the four cell types under the three different surface conditions: HSA (hatched bars), FG (solid bars), and PPP (open bars).

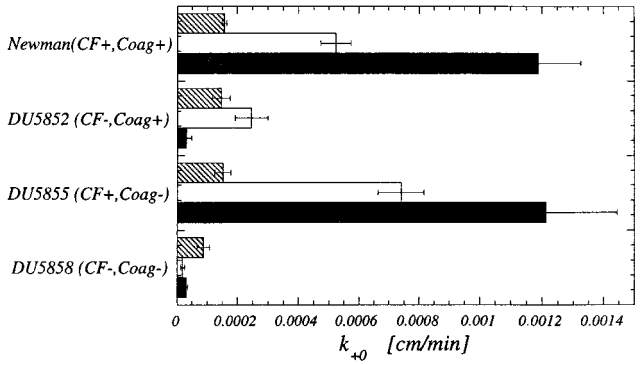

FIG. 5. Base attachment rate constants. The intrinsic attachment rate constant, k_+, was assumed to depend on the shear rate, S, by the relation $k_+ = k_{+0}e^{-\delta S}$, where k_{+0} and δ are fitted parameters. k_{+0} is the base attachment rate constant, the hypothetical zero-shear limit of k_+, and is plotted here for each case corresponding to those shown in Fig. 4.

Here, the shear-averaged value of $\ln(\bar{k}_-)$, $<\ln(\bar{k}_-)>$, was obtained by averaging over shear rates between 1,500 and 7,000 s^{-1}. $<\ln(\bar{k}_-)>$ values for all cell types were similar and were largest on HSA, indicating weakest resistance to detachment on HSA. Therefore, HSA can again be considered the minimally adhesive control surface for detachment. On PPP, $<\ln(\bar{k}_-)>$ was small and similar for both CF-positive cell types, the wild type (CF^+ $Coag^+$) and DU5855 (CF^+ $Coag^-$), and was large and similar for the CF-negative mutants, DU5852 (CF^- $Coag^+$) and DU5858 (CF^- $Coag^-$). These results suggest that CF alone was necessary and sufficient to increase the resistance to detachment on PPP, consistent with the attachment results (compare Fig. 4). However, for FG, the detachment data were more difficult to interpret because $<\ln(\bar{k}_-)>$ for all cell types, including DU5858 (CF^- $Coag^-$), was lower on FG than on HSA, indicating a strong resistance to detachment on FG regardless of the combination of CF and Coag. This is in contrast to the attachment results and suggests that the cells that are attached to FG had an additional adhesion mechanism independent of both CF and Coag that increased the adhesion strength of attached cells; either the presence of fibrinogen increased the nonspecific adhesion interactions or an additional fibrinogen-binding molecule that only increased detachment without aiding attachment was present.

The adhesion energy heterogeneity parameter, σ, showed no significant statistical correlation with shear rate (data not shown). The estimates of σ shown in Fig. 10 were therefore obtained by averaging the values from all shear rates measured. These data show that σ was close to 2.0 for all weakly attached cells surfaces (i.e., all cell types on HSA and CF-negative mutants on PPP) and close to 3.0 for all strongly attached cells, suggesting a greater heterogeneity in adhesion strength on the surfaces where cells were more resistant to detachment.

Noting the generally exponential relationship between $\bar{k}_-$ and S as shown in Fig. 8, the dependence of adhesion strength on shear rate was quantified by defining a detachment shear sensitivity coefficient, δ_d, as the slope of $\ln(\bar{k}_-)$ versus S. In Fig. 11, δ_d is plotted for the conditions shown in Fig. 9 and 10. In comparing the results shown in Fig. 11 with those in Fig. 9, δ_d correlated directly with weaker resistance to detachment on PPP and HSA. However, the adhesion strength on FG appeared to be sensitive to the shear rate for all cell types, with

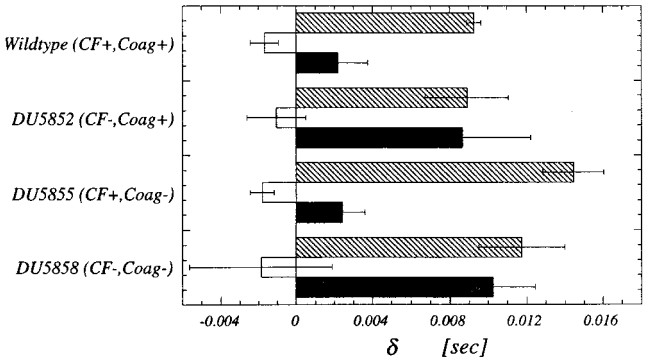

FIG. 6. Shear sensitivity coefficients. The regression estimates of the attachment shear sensitivity coefficient, δ, are plotted for the cases corresponding to those shown in Fig. 4 and 5.

the exception of the most strongly attached cell type, DU5855 (CF^+ $Coag^-$).

DISCUSSION

Depending on the device and application, biomaterials may be exposed to a wide range of shear rates. In the human circulation, for example, shear rates can range between 40 and 2,000 s^{-1} for stable Poiseuille flow in vessels (16), with much higher shear rates possible at vessel entrances, at bifurcations (16), or, for example, in complex flow patterns such as those in heart valves or in the total artificial heart (31). Therefore, stable adhesion requires the ability of the cell to attach and to resist detachment when subjected to a fluid shear force. Full quantitative characterization of the "adhesiveness" requires measuring parameters that reflect the probabilities of the attachment and detachment events. In this study we have defined intrinsic rate constants for both attachment and detachment, k_+ and $\bar{k}_-$, respectively, and have measured these parameters as a function of shear rate. The dependence of these parameters on shear rate is measured by shear sensitivity coefficients for attachment and detachment, δ and δ_d, respectively. Because attached cells showed apparent heterogeneity in resistance to detachment, we also measured the parameter that quantifies this adhesion-energy heterogeneity, σ.

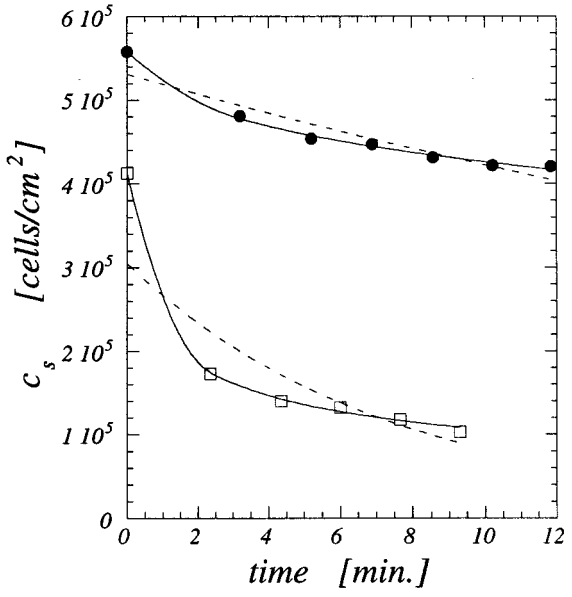

FIG. 7. Detachment kinetics. The surface density of attached bacteria, c_s, is plotted versus time for the detachment of the wild-type strain Newman on FG (circles) or on HSA (squares). The dashed lines represent regression fits of the simple exponential decay model to the data, and the solid lines represent fits of the more general model that accounts for the possibility of heterogeneity in adhesion energy among the attached cell population. The regression analysis yielded estimates for the mean-energy detachment rate constant, $\bar{k}_-$, and the adhesion energy heterogeneity parameter, σ.

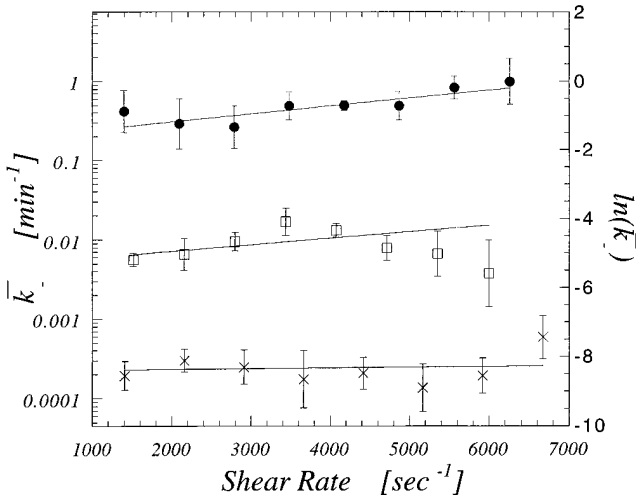

FIG. 8. Detachment rate constants. On a log-linear scale, the mean-energy detachment rate constant, $\bar{k}_-$, is plotted versus the shear rate, *S*, for detachment on HSA (circles), on FG (squares), and on PPP (crosses) for the wild-type strain Newman. The solid lines are the linear least-squares regression fitted lines to the data for $\ln(\bar{k}_-)$ versus *S*.

Measurement of these parameters allowed us to quantify the relative contributions of CF and Coag in mediating *S. aureus* attachment and detachment on fibrinogen-, albumin-, and plasma-coated surfaces as a function of the fluid shear rate. Comparisons of k_+ and $\bar{k}_-$ for the different cell types and surface conditions showed that cell attachment and resistance to detachment were minimized on surfaces coated with human albumin, independent of the presence of CF or Coag; therefore, these molecules apparently do not play a role in nonspecific adhesion to protein-coated surfaces. However, on plasma-coated surfaces, CF was necessary and sufficient to increase the probability of attachment and resistance to detachment; CF-deficient cells had adhesion kinetics similar to those of all cells types on albumin. In contrast, on fibrinogen-coated surfaces, Coag slightly increased the probability of attachment, but this increase was small relative to that afforded by CF alone and apparently was not additive, but perhaps was inhibitory, to the effect of CF when both molecules are present. One possible explanation is that Coag and CF competed for fibrinogen ligands but that the Coag-fibrinogen bond was much weaker than the CF-fibrinogen bond and thus was much less efficient in capturing the cell to the surface. Although there is no previous evidence that cell surface-associated Coag binds directly to surface-adsorbed fibrinogen, previous studies were complicated by the presence of CF. As shown here, the effect of Coag was observed only in the absence of CF. Further studies are required to determine whether cell surface-associated Coag enhances attachment in the absence of CF by binding directly to fibrinogen or by some secondary effect.

As with the attachment results, inexplicable detachment behavior was observed on the fibrinogen-coated surfaces; the

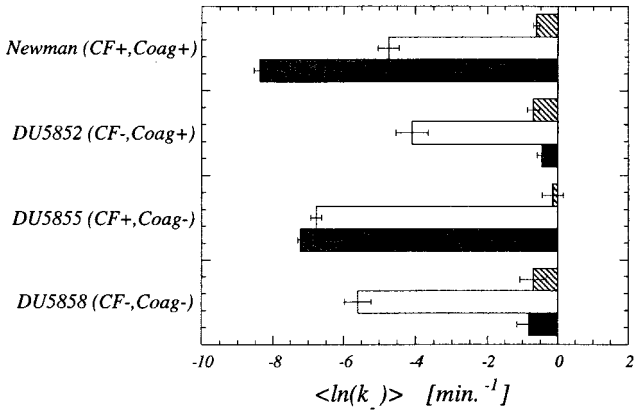

FIG. 9. Shear-averaged detachment rate constants. The shear-averaged values of $\ln(\bar{k}_-)$ are plotted for the four cell types under the three different surface conditions corresponding to those shown in Fig. 4 to 6.

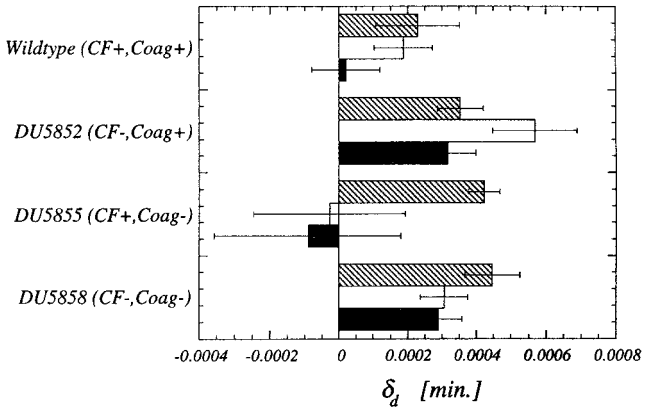

FIG. 11. Detachment shear sensitivity coefficients. The detachment shear sensitivity coefficient, δ_d, is defined as the estimated slope of $\ln(\bar{k}_-)$ versus shear rate (see Fig. 8). The values plotted here were obtained by linear least-squares regression and correspond to the cases shown in Fig. 4 to 6, 9, and 10.

resistance to detachment was large for every strain regardless of the lack of either CF or Coag or both. This result suggests that there may have been involvement of another interaction between the fibrinogen and the bacteria that was independent of both CF and Coag. Because fibrinogen increased the adhesion strength but not k_+ for the double mutant, DU5858 (CF^- $Coag^-$), this interaction appears to have been effective only when the cells were fully attached. Unless fibrinogen somehow indirectly increased the nonspecific interactions between the cell and the surface, this result suggests the possibility of an additional receptor on the Newman strain that bound to purified surface-adsorbed fibrinogen but not to fibrinogen within plasma. If so, one possible scenario could be that its proximity allows its exposure only upon compression of the hydrophilic polysaccharide layer of the cell wall when the cell becomes fully attached to the surface. Possible candidates for this receptor are other *S. aureus* fibrinogen-binding proteins that have recently been isolated (3, 4, 28).

For bacterial adhesion under flow, the sensitivity of the attachment and detachment rate constants to the shear rate is also relevant. Highly shear-sensitive kinetic rate constants would imply that adhesion may be likely under low shear rates but unlikely under high shear rates. From comparison of δ, the probability of attachment was most dependent on shear on albumin-coated surfaces for all cell types and on plasma-coated surfaces for mutants lacking CF. The presence of CF dramatically reduced this shear sensitivity on plasma-coated surfaces. In contrast, on the fibrinogen-coated surfaces, attachment was shear insensitive and possibly even slightly enhanced by shear for all cell types over the range of shear rates measured. This result, coupled with detachment results discussed below, suggests a more complex interaction between the bacteria and purified surface-bound fibrinogen that involves more than just CF and Coag and that does not occur on the plasma form of fibrinogen. Similar to the attachment results, the detachment shear sensitivity coefficient, δ_d, generally correlated with adhesion strength; cells that were most resistant to detachment were generally least sensitive to changes in applied shear. Apparently, the stronger receptor-ligand interactions are insensitive to shear rate relative to nonspecific interactions; therefore, CF may serve not only to enhance the rate of cell attachment, but also to enable cells to resist detachment under high-shear conditions.

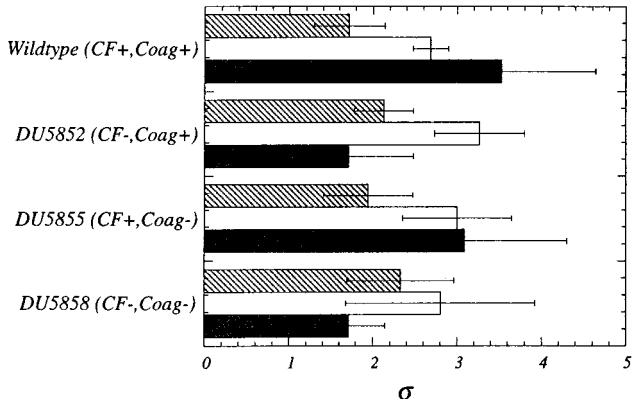

FIG. 10. Adhesion energy heterogeneity parameters. Estimates of the adhesion energy heterogeneity parameter, σ, are plotted for the cases corresponding to those shown in Fig. 4 to 6 and 9. The value for each condition was obtained by (weighted) averaging of the regression estimates of σ over all shear rates measured.

The adhesion energy heterogeneity parameter, σ, was generally larger for cells that were more firmly attached, indicating a greater statistical variance between the adhesion strengths of attached cells. This observation is consistent with some current hypotheses for receptor-mediated adhesion that predict that adhesion governed by small number of higher-energy receptor-ligand bonds will have a statistical variance in the number of bonds among the attached cells, thus resulting in a larger variance in the adhesion energy (7, 35). No such variance is predicted for "smooth" nondiscrete adhesive interactions (35).

Prior to this study, it was unknown whether fibrinogen increased the *S. aureus* adhesion by enhancing the likelihood of cell capture to the surface or by increasing the strength of the adhesion of attached cells. These results suggest a predominant role of CF in increasing both the probability of cell attachment and the resistance to detachment of *S. aureus* Newman on surface-bound fibrinogen and plasma. Although other studies have suggested a role of other plasma proteins in enhancing *S. aureus* attachment to other plasma proteins (10, 21, 22, 28), we have observed here that removal of CF alone is necessary and sufficient to remove any increase of attachment probability or adhesion strength of the Newman strain on the plasma-coated surfaces. This would suggest a minimal role of other plasma proteins in mediating adhesion *S. aureus* New-

man under the experimental conditions used here. The results also suggest that the attachment and detachment mechanisms may differ on purified surface-bound fibrinogen and on fibrinogen adsorbed from its native plasma. The results shown here are likely to partially depend on the material substrate used (glass) or the protein exposure time, which are known to affect the relative quantity or conformation of adsorbed plasma proteins (1, 33). Further studies are required to address the roles of these parameters in receptor-mediated attachment and detachment of *S. aureus* on biomaterial surfaces.

ACKNOWLEDGMENTS

We thank Dorothy Brar, Department of Medical Microbiology, University of Wisconsin—Madison, for assistance with bacterial strain maintenance. Fibrinogen was purified by Jui-Che Lin, Department of Chemical Engineering, University of Wisconsin—Madison.

This work was supported by Public Health Service grant BCS-91-20660, provided jointly by the National Science Foundation and the National Heart, Lung, and Blood Institute. Funding for T.J.C. was provided separately by United Kingdom project no. 033403.

REFERENCES

1. **Andrade, J. D., and V. Hlady.** 1987. Plasma protein adsorption: the big twelve. Ann. N.Y. Acad. Sci. **516:**158–172.
2. **Boden, M. K., and J. I. Flock.** 1989. Fibrinogen-binding protein/clumping factor from *Staphylococcus aureus*. Infect. Immun. **57:**2358–2363.
3. **Boden, M. K., and J. I. Flock.** 1992. Evidence for three different fibrinogen-binding proteins with unique properties from Staphylococcus aureus strain Newman. Microb. Pathog. **12:**289–298.
4. **Boden, M. K., and J. L. Flock.** 1994. Cloning and characterization of a gene for a 19 kDa fibrinogen-binding protein from *Staphylococcus aureus*. Mol. Microbiol. **12:**599–606.
5. **Bruckler, J., W. Schaeg, and H. Blobel.** 1974. Isolation of 'clumping factor' of *Staphylococcus aureus*. Zentralbl. Bakteriol. Mikrobiol. Hyg. Ser. A **228:** 465–473.
6. **Cheung, A. L., and V. A. Fischetti.** 1990. The role of fibrinogen in staphylococcal adherence to catheters *in vitro*. J. Infect. Dis. **161:**1177–1186.
7. **Cozens-Roberts, C., D. A. Lauffenburger, and J. A. Quinn.** 1990. Receptor-mediated cell attachment and detachment kinetics. I. Probabilistic model and analysis. Biophys. J. **58:**841–856.
8. **Dankert, J., A. H. Hogt, and J. Feijen.** 1986. Biomedical polymers: bacterial adhesion, colonization, and infection. Crit. Rev. Biocompat. **2:**219–301.
9. **Davison, V. E., and B. A. Sandford.** 1982. Factors influencing adherence of *Staphylococcus aureus* to influenza A virus-infected cell cultures. Infect. Immun. **37:**946–955.
10. **Delmi, M., P. Vaudaux, D. P. Lew, and H. Vasey.** 1994. Role of fibrinogen in staphylococcal adhesion to metallic surfaces used as models of orthopaedic devices. J. Orthop. Res. **12:**432–438.
11. **Dickinson, R. B., and S. L. Cooper.** Quantitative measurement and mathematical analysis of shear-dependent bacterial adhesion kinetics to biomaterial surfaces. Am. Inst. Chem. Eng. J., in press.
12. **Dougherty, S. H.** 1988. Pathobiology of infection in prosthetic devices. Rev. Infect. Dis. **10:**1102–1117.
13. **Duthie, E. S., and L. L. Lorenz.** 1952. Staphylococcal coagulase: mode of action and antigenicity. J. Gen. Microbiol. **6:**95–107.
14. **Espersen, F., I. Clemmensen, and V. Barkholt.** 1985. Isolation of *Staphylococcus aureus* clumping factor. Infect. Immun. **49:**700–708.
15. **Fowler, H. W., and A. J. McKay.** 1980. The measurement of microbial adhesion. p. 143–161. *In* R. C.W. Berkeley et al. (ed.), Microbial adhesion to surfaces. Ellis Horwood Limited, Chichester, England.
16. **Goldsmith, H. L., and V. T. Turitto.** 1986. Rheological aspects of thrombosis and haemostasis: basic principles and applications. Thromb. Haemost. **55:** 415–435.
17. **Gristina, A. G.** 1987. Biomaterial-centered infection: microbial adhesion versus tissue integration. Science **237:**1588–1595.
18. **Gristina, A. G., C. D. Hobgood, and E. Barth.** 1987. Biomaterial specificity, molecular mechanisms and clinical relevance of *S. epidermidis* and *S. aureus* infections in surgery. Zentralbl. Bakteriol. Suppl. **16:**143–157.
19. **Hawiger, J., M. Kloczewiak, S. Timmons, D. Strong, and R. F. Doolittle.** 1983. Interaction of fibrinogen with staphylococcal clumping factor and with platelets. Ann. N.Y. Acad. Sci. **408:**521–535.
20. **Hawiger, J. S., D. K. Hammond, S. Timmons, and A. Z. Budzynski.** 1978. Interaction of human fibrinogen with staphylococci: presence of a binding region on normal and abnormal fibrinogen variants and fibrinogen derivatives. Blood **51:**799–812.
21. **Herrmann, M., Q. J. Lai, R. M. Albrecht, D. F. Mosher, and R. A. Proctor.** 1993. Adhesion of *Staphylococcus aureus* to surface-bound platelets: role of fibrinogen/fibrin and platelet integrins. J. Infect. Dis. **167:**312–322.
22. **Herrmann, M., P. E. Vaudaux, D. Pittet, R. Auckenthaler, P. D. Lew, F. Schumacher-Perdreau, G. Peters, and F. A. Waldvogel.** 1988. Fibronectin, fibrinogen, and laminin act as mediators of adherence of clinical staphylococcal isolates to foreign material. J. Infect. Dis. **158:**693–701.
23. **Hogg, R. V., and E. A. Tanis.** 1983. Probability and statistical inference, 2nd ed. Macmillan Publishing Co., Inc., New York.
24. **Kuusela, P., T. Vartio, M. Vuento, and E. B. Myhre.** 1984. Binding sites for streptococci and staphylococci in fibronectin. Infect. Immun. **45:**433–436.
25. **Kuusela, P., T. Vartio, M. Vuento, and E. B. Myhre.** 1985. Attachment of staphylococci and streptococci on fibronectin, fibronectin fragments, and fibrinogen bound to a solid phase. Infect. Immun. **50:**77–81.
26. **McDevitt, D., P. Francois, P. Vaudaux, and T. J. Foster.** 1994. Molecular characterization of the clumping factor (fibrinogen receptor) of *Staphylococcus aureus*. Mol. Microbiol. **11:**237–248.
27. **McDevitt, D., P. Vaudaux, and T. J. Foster.** 1992. Genetic evidence that bound coagulase of *Staphylococcus aureus* is not clumping factor. Infect. Immun. **60:**1514–1523.
28. **McGavin, M. H., P. D. Krajewska, C. Ryden, and M. Hook.** 1993. Identification of a *Staphylococcus aureus* extracellular matrix-binding protein with broad specificity. Infect. Immun. **61:**2479–2485.
29. **Mohammad, S. F., N. S. Topham, G. L. Burns, and D. B. Olsen.** 1988. Enhanced bacterial adhesion on surfaces pretreated with fibrinogen and fibronectin. Trans. Am. Soc. Artif. Intern. Organs **34:**573–577.
30. **Moller, P. S.** 1963. Radial flow without swirl between parallel discs. Aeronautical Q. **14:**163–186.
31. **National Aeronautics and Space Administration.** 1989. Numerical stimulation of flow through an artificial heart. NASA Report. Ames Research Center, National Aeronautics and Space Administration, Ames, Iowa.
32. **Ohtomo, T., and K. Yoshida.** 1988. Adhesion of *Staphylococcus aureus* to fibronigen, collagen, and lectin in relation to cell surface structure. Zentralbl. Bakteriol. Mikrobiol. Hyg. Ser. A **268:**325–340.
33. **Pitt, W. G., K. Park, and S. L. Cooper.** 1986. Sequential protein adsorption and thrombus deposition on polymeric biomaterials. J. Coll. Interf. Sci. **111:**343–362.
34. **Proctor, R. A., D. F. Mosher, and P. J. Olbrantz.** 1982. Fibronectin binding to *Staphylococcus aureus*. J. Biol. Chem. **257:**14788–14794.
35. **Saterbak, A., S. C. Kuo, and D. A. Lauffenburger.** 1993. Heterogeneity and probabilistic binding contributions to receptor-mediated cell detachment kinetics. Biophys. J. **65:**243–252.
36. **Seber, G. A. F., and C. J. Wild.** 1989. Nonlinear regression. John Wiley & Sons, New York.
37. **Switalski, L. M.** 1976. Isolation and purification of staphylococcal clumping factor, p. 413–425. *In* J. Jeljaszewicz (ed.), Staphylococci and staphylococcal diseases. Gustav Fischer Verlag, Stuttgart, Germany.
38. **Usui, Y.** 1985. Biochemical properties of fibrinogen binding protein (clumping factor) of staphylococcal cell surface. Zentralbl. Bakteriol. Mikrobiol. Hyg. Ser. A **262:**287–297.
39. **Vaudaux, P., R. Suzuki, F. A. Waldvogel, J. J. Morgenthaler, and U. E. Nydegger.** 1984. Foreign body infection: role of fibronectin as a ligand for the adherence of *Staphylococcus aureus*. J. Infect. Dis. **150:**546–553.
40. **Vaudaux, P., H. Yasuda, M. I. Velazco, E. Huggler, I. Ratti, F. A. Waldvogel, D. P. Lew, and R. A. Proctor.** 1990. Role of host and bacterial factors in modulating staphylococcal adhesion to implanted polymer surfaces. J. Biomater. Appl. **5:**134–153.